Thermal activation of As implanted in bulk Si and separation by implanted oxygen

M. Dalponte[a)] and H. Boudinov
Instituto de Física, Universidade Federal do Rio Grande do Sul, 91501-970, Porto Alegre-RS, Brazil

L. V. Goncharova, D. Starodub, E. Garfunkel, and T. Gustafsson
Department of Physics and Astronomy and Laboratory for Surface Modification, Rutgers University, 136 Frelinghuysen Road, Piscataway, New Jersey 08854-8019

(Received 30 March 2004; accepted 2 June 2004)

We have studied arsenic (As) diffusion and its electrical activation in two different types of silicon substrates: bulk Si and separation by implanted oxygen (SIMOX) wafers. Both substrates were implanted with a dose of 5×10^{14} cm^{-2} As^{+} at 20 keV. The samples were annealed and physical characterization was performed with secondary ion mass spectrometry (SIMS), Rutherford backscattering spectrometry, and medium energy ion scattering. The electrical properties of the film were extracted by Hall measurements. The SIMS results showed a lower dopant outdiffusion loss to the atmosphere during annealing in the SIMOX samples. The electrical results for the SIMOX samples were also superior to those of bulk Si due to the higher dopant retention, likely the result of a higher concentration of vacancies, which in turn increases the relative fraction of As which is activated (in substitutional sites). The net effect was a higher sheet carrier concentration and lower sheet resistance in the SIMOX samples. The implantation damage removal was superior in SIMOX samples compared to bulk Si ones. © *2004 American Institute of Physics.*
[DOI: 10.1063/1.1776319]

I. INTRODUCTION

Silicon-on-insulator (SOI) based devices are superior to those made on bulk Si primarily because of better isolation.[1,2] Of all the ways to prepare SOI substrates, Separation by Implanted Oxygen (SIMOX) has received the most attention. A wide range of SIMOX fabrication processing routes have been explored with thorough characterization of the SOI and Buried OXide (BOX) layers.[3–6] In addition to developing a general understanding of the silicon film and BOX properties, the dopant behavior within this material is also of great importance. This is particularly true for ultrashallow junction fabrication, where highly doped, highly activated, and low sheet resistance films must be obtained.[7] In this scenario, diffusion of dopants and their interaction with defects can have drastic effects on device performance.[8,9] It is well established that in SIMOX there are residual point defects, mainly vacancy-oxygen complexes.[3–6] It is also known that As strongly interacts with vacancies, creating As_nV complexes. The higher the initial As concentration, the faster the complex formation and the larger the complexes (larger n), since there are more available As atoms for this process. These complexes are less mobile during annealing than the isolated dopant itself.[10] Therefore, one would expect that As-doped SIMOX would show less dopant loss to the atmosphere during annealing than bulk Si.

When bonded to a vacancy, the As atoms are electrically inactive. Furthermore, Xie and Chen showed.[10] that the interaction between As and a vacancy is affected by other As atoms located as far away as the ninth nearest neighbor, which can be electrically active dopants. In other words, the diffusion of all As atoms closer than the ninth neighbor will be affected by the presence of that AsV complex. Experiments suggest that a large fraction of electrically inactive As atoms are either in substitutional lattice sites in the form of As clusters,[11] or, for high dopant concentrations, coherent crystalline precipitates.[12,13] The latter are expected to be present both in bulk Si and SIMOX, although the clusters containing vacancies should be favored in SIMOX compared to bulk Si due to the higher vacancy concentration in this type of substrate.

In this paper we compare the As dopant behavior in bulk Si and SIMOX with special consideration of the above mentioned effects. We have studied the dopant profiles and electrical characteristics in both types of substrates before and after annealing.

II. EXPERIMENTAL DETAILS

The experiments were performed on (100) oriented p-type substrates with a resistivity of 11 Ω cm for both bulk Si and SIMOX. Standard SIMOX substrates with a 0.20 μm Si overlayer and a 0.36 μm buried SiO_2 layer were used. Native SiO_2 was removed in diluted HF just before ion implantation. As^{+} implantation on both substrates was performed with an energy of 20 keV and a dose of 5×10^{14} cm^{-2}. The samples were then processed using rapid thermal annealing (RTA) at 1000 °C for 10 s or furnace annealing (FA) at 950 °C for 15 min in a nitrogen ambient.

Rutherford backscattering spectrometry (RBS) spectra were obtained with a 1.2 MeV He^{+} beam in random and channeled (100) directions with the detector positioned at 170° from the incident beam. Additional RBS channeling

a)Electronic mail: dalponte@if.ufrgs.br

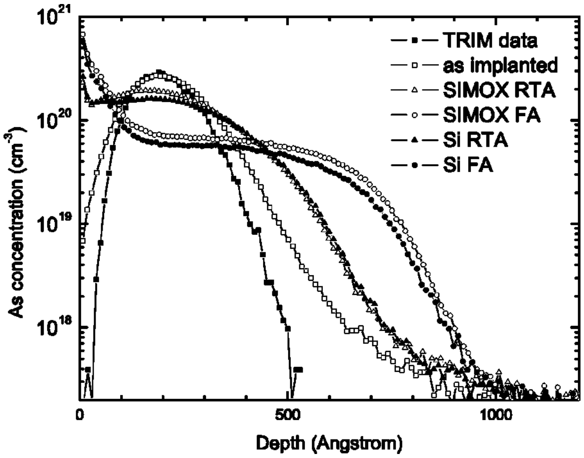

FIG. 1. SIMS profiles of As implanted Si with a dose of 5×10^{14} cm^2 at 20 keV in SIMOX and bulk Si. Dopant distributions before and after annealing are presented. A TRIM profile is also shown for comparison.

experiments at 2.0, 1.2, 0.8, and 0.4 MeV were performed to measure the channel width of the bulk Si samples after the different annealing processes. The medium energy ion scattering (MEIS) measurements utilized a H^+ beam with energy of 99 keV. Backscattered ion energies were analyzed with a high-resolution ($\Delta E/E \sim 0.1\%$) toroidal electrostatic energy detector. Depth profiles of the elements were obtained from simulations of the backscattered ion energy distribution. Both random and channeling scattering geometries were used. Secondary ion mass spectrometry (SIMS) was performed with O_2^+ as the primary ion and an effective incidence energy of 3.5 keV. The samples that were used for electrical measurements were patterned by photolithography to create a van der Pauw structure prior to As^+ implantation. Sheet resistance and Hall measurements were performed using a magnetic field of ~0.3T. Currents in the range from 0.5 mA to 15 mA were applied to the As doped layer to extract the electrical data.

III. RESULTS AND DISCUSSION

Figure 1 shows the As profiles in all samples, as measured by SIMS, and also includes a TRIM simulated profile for the relevant incident energy. The As as-implanted profiles in the bulk Si and SIMOX are similar, so only one of them is shown. Clearly, after annealing the As concentration is slightly higher in the SIMOX samples than in the bulk Si ones. This effect might be caused by the presence of vacancies in the SOI layer, which retain the As atoms inside the material, since it is energetically more favorable for As to bind to a vacancy than to a Si atom.[14] The largest difference in the As concentration for the RTA samples (~19%) is located at the projected range of the as-implanted profile, which is a region of higher probability of As clustering (or complex formation) due to the high dopant concentration. We can also observe dopant migration towards the surface, mainly in the FA samples, in which the dopant concentration reached values above the solubility limit in the near surface region.[15] The high dopant concentration on the surface also

TABLE I. Physical and electrical characteristics of As implanted with a dose of 5×10^{14} cm^{-2} at 20 keV in bulk Si and SIMOX after RTA (1000 °C/10 s) and FA (950 °C/15 min).

	Restained dose (SIMS) cm^{-2}	(SIMS) %	Sheet concentration cm^{-2}	Activation %	Carrier Mobility cm^{-2}/V.s	Sheet resistance Ω/□
SIMOX RTA	4.7×10^{14}	94	4.7×10^{14}	100	59	225 ± 1
SIMOX FA	4.4×10^{14}	88	2.9×10^{14}	66	73	292 ± 1
Si RTA	4.4×10^{14}	88	4.3×10^{14}	98	63	231 ± 2
Si FA	3.6×10^{14}	72	2.7×10^{14}	75	75	307 ± 2

led to a high dopant loss to the atmosphere during annealing. It is interesting to note that the dopant loss in SIMOX was about half of that in bulk Si (see Table I).

Selected physical and electrical results for the annealed samples are presented in Table I. The retained As dose after annealing and the percentage it represents in terms of the implanted dose are shown in the first two columns. The values were obtained by integrating the SIMS profiles. The other columns summarize the Hall measurement data. The activation percentage was calculated as the ratio of the sheet carrier concentration to the retained dopant dose. The electrical characteristics are directly correlated to the dopant annealing behavior, i.e., we observe that the SIMOX samples exhibit lower sheet resistance (due to the higher dopant concentration) than the bulk Si samples. This difference becomes more clear if we compare results for the FA samples. Bulk Si samples show higher dopant activation values, but since the total dopant concentration is lower (by ~19%, from 200 to 550 A), the net result is a lower sheet carrier concentration and a higher value of the sheet resistance. We propose that this is due to the formation of As_nV complexes in SIMOX. The FA samples show a more pronounced effect due to the longer annealing time, which allows the formation of a larger number of these complexes. For longer annealing times the As_nV complex concentration increases as well as the As fraction in them, which means increasing n.[10] As mentioned previously,[11] As atoms are electrically inactive when bound to a vacancy. This dopant deactivation process is most significant after the implantation damage has been removed by annealing and when the dopants start to form complexes with vacancies and clusters.[10,11]

Another interesting feature is the lower damage level in the SIMOX samples after RTA compared to bulk Si, as can be seen in the RBS channeled spectrum of the As peak in Fig. 2(a). The SIMOX channeled spectrum yield is very low, which is indicative of good As substitutionality in the Si lattice of the SOI layer. In the bulk Si the yield is also low, but higher than in SIMOX, showing more defects in the bulk Si samples. These defects consist of As atoms displaced from Si lattice positions, increasing the backscattered particle yield in channeling. We suggest that the As atoms in the SIMOX samples are more easily incorporated into the lattice in the first moments of annealing due to the presence of vacancies, but after longer annealing times, as we see for the FA samples of Fig. 2(b), the spectra become similar. This

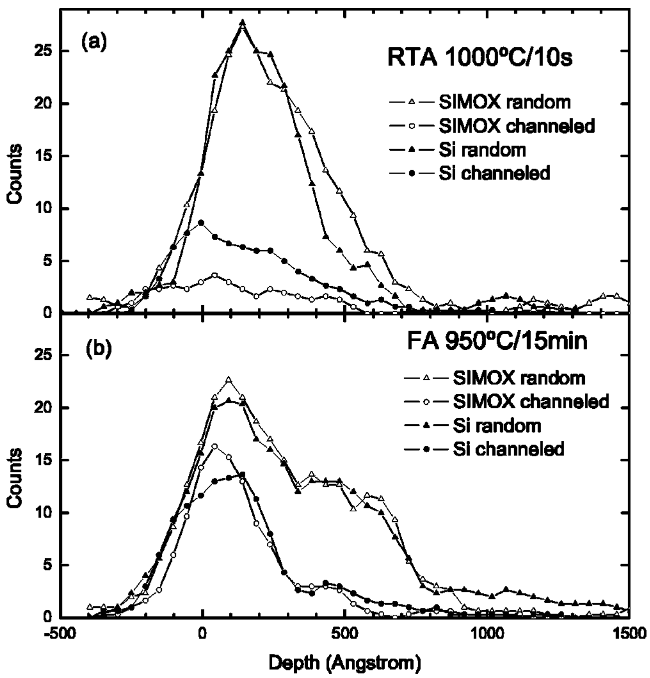

FIG. 2. RBS profiles of the As peak in random and channeled directions in SIMOX and bulk Si. Dopant distributions are shown after RTA (a) and FA (b).

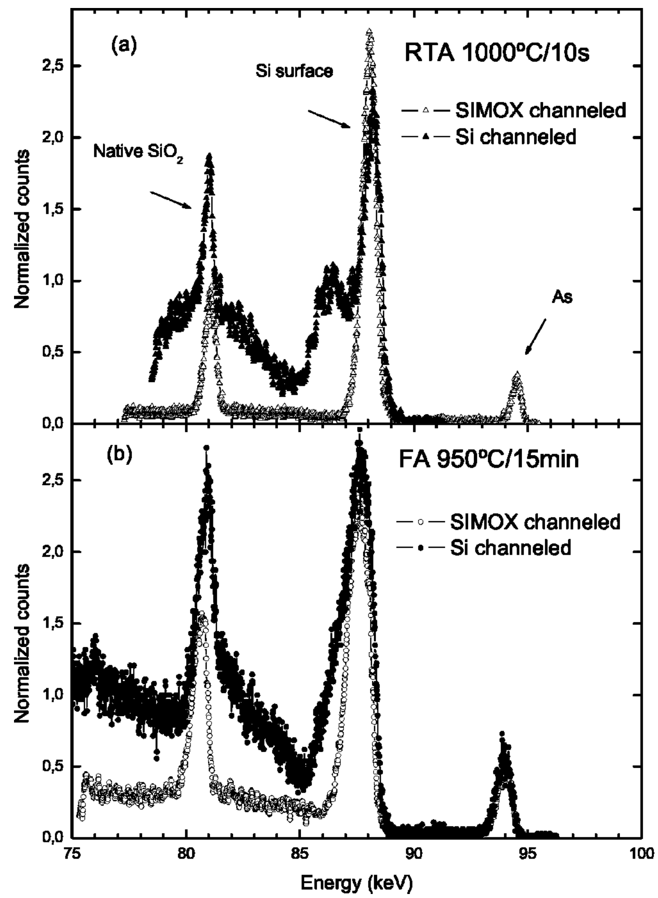

FIG. 3. MEIS spectra of 20 keV As^+ ions implanted into bulk Si (solid symbols) and SIMOX (open symbols) to a dose of 5×10^{14} cm^{-2} and followed by (a) RTA and (b) FA treatments. Channeled spectra are shown as measured at a scattering angle of 125°.

shows that the lattice reconstruction process is similar for both SIMOX and bulk Si, i.e., the vacancies should not play an important role for longer times or higher temperatures. The higher yields of both channeled FA samples compared to the RTA ones will be discussed below.

The electrical activation of RTA samples (see Table I) was very similar in both substrates, with the SIMOX values being slightly superior. It might be caused by the better arrangement of dopants in the Si lattice, as shown in Fig. 2(a). As shown earlier,[16] in the first stage of annealing the activation is dominated by ion implantation damage recovery. When the damage is completely annealed out, the dopants reach the maximum electrical activation. If the annealing is continued longer, deactivation processes begin to dominate. As_nV complexes and clusters start to form.[10] The As atoms involved in those defects will no longer be electrically active, explaining the lower activation measured in the FA SIMOX samples compared to the FA bulk Si samples. The difference in the activation results between the two substrates is attributed to the presence of excess vacancies in SIMOX.

The MEIS spectra presented in Fig. 3 indicate that there is a significant reordering of the initially damaged Si layers. The Si peak for the as-implanted sample (not shown here) reaches the height, characteristic of random ion incidence. It extends to a depth of >25 nm implying formation of an amorphous Si layer. Comparison of surface Si peaks for samples after RTA [Fig. 3(a)] and FA [Fig. 3(b)] indicates that the damage level in the Si crystal lattice is higher in the bulk Si samples. The RTA treated bulk Si sample exhibits two additional peaks besides the surface peak. One corresponds to a defect layer located at a depth of about 7 nm (at 86 keV), that is, formed by interstitial Si atoms trapped during the annealing[17] and the third peak corresponds to Si atoms involved in defects at the implantation projected range, at a depth of about 29 nm (at 81 keV). Neither of these two peaks are observed in the RTA SIMOX sample. This sample has the lowest yield in the Si subsurface region, corresponding to the best lattice reordering, being practically that of an undamaged sample after the annealing. The absence of the second peak in the RTA SIMOX sample confirms that the vacancies play an important role in annihilating the interstitials generated during ion implantation and annealing. In neither of the FA samples is the distinct second peak visible; however the interstitials have diffused in the FA bulk Si samples, resulting in a wider Si surface peak, due to the larger depth distribution that occurs during the long annealing time. In the FA SIMOX samples the vacancies are responsible for decreasing the accumulation of interstitials. The same effect is observed in the RTA SIMOX samples. In addition, similar As peaks are observed for both FA samples, indicating the same level of displaced dopant atoms accumulating in the near surface region. The As surface peak is slightly lower in the RTA SIMOX sample showing better substitutionality of dopants in the Si lattice.

Figure 4 presents RBS channeling minimum yield angular scans in the (100) direction for unimplanted, RTA and FA annealed bulk Si samples. For brevity only the spectrum for 0.4 MeV beam energy is shown. One can see different full width at half maximum (FWHMs) of the channel width, de-

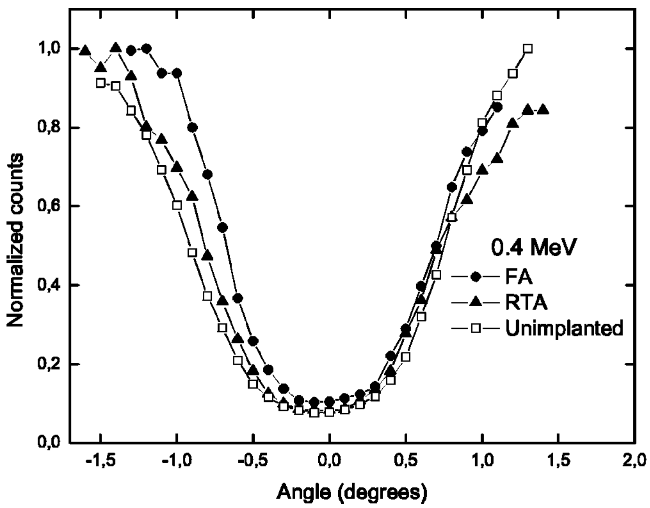

FIG. 4. RBS channeling minimum yield angular scans in the (100) direction for unimplanted, RTA and FA annealed Si samples.

pending on which thermal process the sample experienced. Figure 4 shows also that the RTA (100) channel scan is closer to the unimplanted original Si sample, due to a better lattice reconstruction, compared to the FA. The narrowest channel is found in the FA samples, confirming that the average displacement of the Si atoms towards the center of the channel is the largest in this case. The calculated As-Si bond lengths are typically 2% larger than Si-Si bonds; the formation of As clusters may cause this lattice distortion.[14] It is important to note that the crystal channels are not blocked in any of the annealed samples, i.e., the dopants are substitutional, only their average channel width is different for different annealing conditions.

IV. CONCLUSIONS

We have performed As ion implantation in two different substrates, SIMOX and bulk Si. After RTA annealing, the SIMOX samples showed superior performance over the bulk Si ones: better dopant substitutionality, higher dopant concentration and activation, and lower sheet resistance. After FA annealing, the SIMOX and bulk Si samples presented similar dopant substitutionality. However, the SIMOX samples showed a higher dopant concentration and lower sheet resistance, even though the dopant activation was lower than in bulk Si. The differences in dopant profile and electrical activation were attributed to the presence of vacancies in the SOI film and their interaction with the As atoms. Also, RTA annealing is shown to be superior compared to FA from the viewpoint of lattice reconstruction. We attribute this to the formation of As clusters in FA samples due to the longer annealing time. The existence of a vacancy rich layer in the SIMOX samples significantly improves damage recovery and dopant arrangement in the Si crystal lattice during thermal treatment.

ACKNOWLEDGMENTS

This work was partially supported by Conselho Nacional de Desenvolvimento Científico e Tecnológico (CNPq) and Fundação de Amparo à Pesquisa do Estado do Rio Grande do Sul (FAPERGS), by the US National Science Foundation under Grant No. DMR- DMR 0218406, by the Semiconductor Research Corporation, and by Sematech International.

[1] S. Cristoloveanu and S. S. Li, *Electrical Characterization of SOI Materials and Devices* (Kluwer Academic, Boston, 1995).
[2] J. P. Colinge, *SOI Technology: Materials to VLSI* (Kluwer Academic, Boston, 1997).
[3] E. C. Jones and E. Ishida, Mater. Sci. Eng., R. **24**, 1 (1998).
[4] T. O. Sedgwick, Nucl. Instrum. Methods Phys. Res. B **37/38**, 760 (1989).
[5] S. Moffatt, P. L. F. Hemment, S. Whelan, and D. G. Armour, Mater. Sci. Semicond. Process. **3**, 291 (2000).
[6] A. C. Kruseman, H. Schut, A. van Veen, and M. Fujinami, Nucl. Instrum. Methods Phys. Res. B **148**, 294 (1999).
[7] A. Uedono, Z. Q. Chen, A. Ogura, R. Suzuki, T. Ohdaira, and T. Mikado, J. Appl. Phys. **91**, 6488 (2002).
[8] Z. Q. Chen, A. Uedono, A. Ogura, H. Ono, R. Suzuki, T Ohdaira, and T Mikado, Appl. Surf. Sci. **194**, 112 (2002).
[9] S. L. Ellingboe and M. C. Ridgway, Mater. Sci. Eng., B **29**, 29 (1995).
[10] J. Xie and S. P. Chen, Phys. Rev. Lett. **83**, 1795 (1999).
[11] H. Kobayashi, I. Nomachi, S. Kusanagi, and F. Nishiyama, Nucl. Instrum. Methods Phys. Res. B **190**, 547 (2002).
[12] S. Whelan, V. Privitera, G. Mannino, M. Italia, C. Bongiorno, A. La Magna, and E. Napolitani, J. Appl. Phys. **90**, 3873 (2001).
[13] V. Krishnamoorthy, K. Moller, K. S. Jones, D. Venables, J. Jackson, and L. Rubin, J. Appl. Phys. **84**, 5997 (1998).
[14] J. Xie and S. P. Chen, J. Appl. Phys. **87**, 4160 (2000).
[15] E. Guerrero, H. Potzl, R. Tielert, M. Grasserbauer, and G. Stingeder, J. Electrochem. Soc. **129**, 1826 (1982).
[16] S. Solmi, M. Attari, and D. Nobili, Appl. Phys. Lett. **80**, 4774 (2002).
[17] J. P. de Souza, P. F. P. Fichtner, and D. K. Sadana, in *Rapid Thermal and Integrated Processing III*, edited by J. J. worbman, J. C. Gelpey, M. L. Green, S. R. J. Brueck, and F. Roozeleoom, MRS Symposia Proceedings, No. 342 (Materials Research Society, Pittsburgh, 1994).